
Using MCP6491 Op Amps for Photodetection Applications

Author: Yang Zhen
Microchip Technology Inc.

INTRODUCTION

Low input bias operational amplifiers (op amps) are often required for a wide range of photodetection applications, in order to reduce current error and improve the accuracy of the output signal.

The typical photodetection applications are listed below:

- Smoke Detectors
- Flame Monitors
- Airport Security X-Ray Scanners
- Light Meters
- Brightness Controls
- Bar Code Scanners
- Pulse Oximeters
- Blood Particle Analyzers
- CT Scanners
- Automotive Headlight Dimmers
- Twilight Detectors
- Photographic Flash Controls
- Automatic Shutter Controls
- Optical Remote Controls
- Optical Communications, etc.

This application note discusses the features of Microchip's MCP6491 low input bias current op amps [1], the characteristics of photodiodes, and the strengths of the active photodiode current-to-voltage converter (i.e. photodiode amplifier), compared to the passive version. Next, the focus shifts to the design techniques of photodiode amplifier circuitry. Several key design points are discussed in order to improve the circuit's performance. Then, a practical application example with PSpice simulation results is provided, to help illustrate the design techniques in depth. In addition, the noise analysis of the photodiode amplifier and the design of a companion low pass filter are discussed. Finally, the PCB techniques that help reduce the current leakage are briefly introduced.

MCP6491 LOW INPUT BIAS CURRENT OP AMPS

Microchip's MCP6491 family of op amps has low input bias current (150 pA, typical at 125°C) and rail-to-rail input and output operation. The MCP6491 family is unity gain stable and has a gain bandwidth product of 7.5 MHz (typical). These devices operate with a single-supply voltage as low as 2.4V, while only drawing 530 μ A/amplifier (typical) of quiescent current. These features make the MCP6491 family of op amps well suited for photodiode amplifier, pH electrode amplifier, low leakage amplifier, and battery-powered signal conditioning applications, etc.

Features:

- Low Input Bias Current
 - ± 1 pA (typical at 25°C)
 - 8 pA (typical at 85°C)
 - 150 pA (typical at 125°C)
- Low Quiescent Current:
 - 530 μ A/amplifier (typical)
- Low Input Offset Voltage:
 - ± 1.5 mV (maximum)
- Rail-to-Rail Input and Output
- Supply Voltage Range: 2.4V to 5.5V
- Gain Bandwidth Product: 7.5 MHz (typical)
- Slew Rate: 6 V/ μ s (typical)
- Unity Gain Stable
- No Phase Reversal
- Small Packages
 - Singles in SC70-5, SOT-23-5
- Extended Temperature Range
 - -40°C to +125°C

Related Parts

- MCP6481: 4 MHz, Low Input Bias Current Op Amps [2]
- MCP6471: 2 MHz, Low Input Bias Current Op Amps [3]

PHOTODETECTION APPLICATIONS

There are many detectors which can be used for photodetection applications, such as photodiodes, phototransistors, photoresistors, phototubes, photomultiplier tubes, charge-coupled devices, etc.

In this application note, we will focus on the photodiode, as it is the most common photodetector and widely used for the detection of intensity, position, color and presence of light.

Photodiode

The photodiode is a type of photodetector capable of converting light to a small current which is proportional to the level of illumination.

FEATURES

The photodiode's features can be summarized as below:

- Wide spectral response
- Excellent linearity
- Low noise
- Excellent ruggedness and stability
- Small physical size
- Long lifetime
- Low cost

EQUIVALENT CIRCUIT

The equivalent circuit for a photodiode is shown below, in [Figure 1](#).

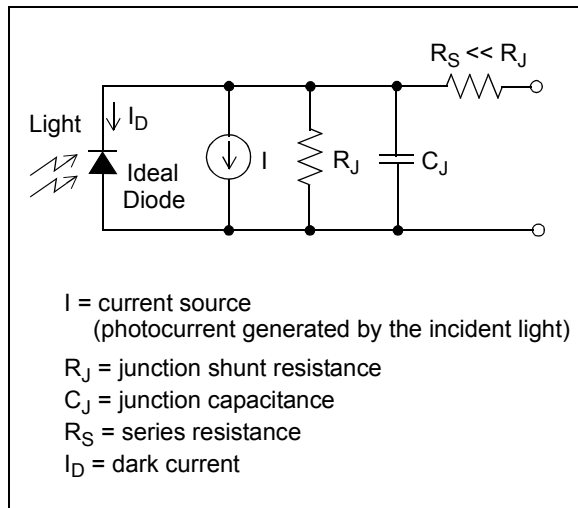


FIGURE 1: A Photodiode Equivalent Circuit.

A photodiode can be represented by a current source (I), a junction shunt resistance (R_J), and a junction capacitance (C_J) in parallel with an ideal diode. The series resistance (R_S) is connected with all other components in series. Dark current (I_D) only exists under reverse bias conditions.

- Junction Shunt Resistance (R_J)

R_J represents the resistance of the zero-biased photodiode junction. An ideal photodiode will have an infinite R_J , but the actual value of R_J is typically on the order of thousands of $M\Omega$, which depends on the photodiode material, and decreases by a factor of 2 for every 10°C rise in temperature. The high value of R_J yields the low noise current of the photodiode.

- Series Resistance (R_S)

R_S is the resistance of the wire bonds and contacts of the photodiode. An ideal photodiode should have no series resistance, but the typical value is on the order of tens of Ω , which is much smaller than R_J . The R_S is used to determine the linearity of the photodiode under zero bias conditions. For most of applications, it can be ignored.

- Junction capacitance (C_J)

C_J is directly proportional to the junction area and inversely proportional to the diode reverse bias voltage. For a small area diode at zero bias, the typical value is on the order of tens of pF.

- Dark Current (I_D)

I_D is the small leakage current that flows through photodiode under reverse bias conditions. It exists even when there is no illumination and approximately doubles for every 10°C rise in temperature. There is no dark current under zero bias conditions.

OPERATION MODES

There are two operation modes for the photodiode, the photovoltaic mode and the photoconductive mode, as shown in [Figure 2](#) and [Figure 3](#). The two modes have their own strengths and drawbacks, and mode selection is dependent on the target application.

- Photovoltaic Mode

This mode has zero voltage potential across the photodiode. No dark current flows through the photodiode, the linearity and sensitivity are maximized, and the noise level is relatively low (R_J 's thermal noise only), which make it well suited for precision applications.

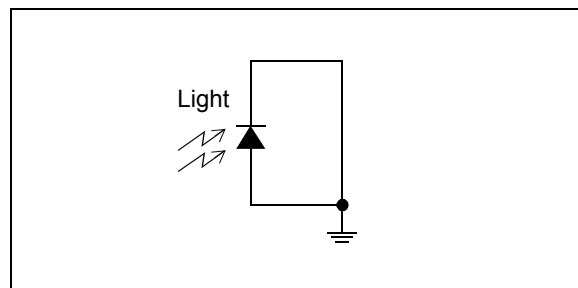


FIGURE 2: Photovoltaic Mode.

- Photoconductive Mode

This mode has a reverse bias voltage placed across the photodiode. The reverse bias voltage reduces the diode junction capacitance and shortens the response time. Therefore, the photoconductive mode is suitable for high speed applications (e.g., high speed digital communications). The main drawbacks of this mode include dark current appearance, non-linearity, and high noise level (R_j 's thermal noise and I_D 's shot noise).

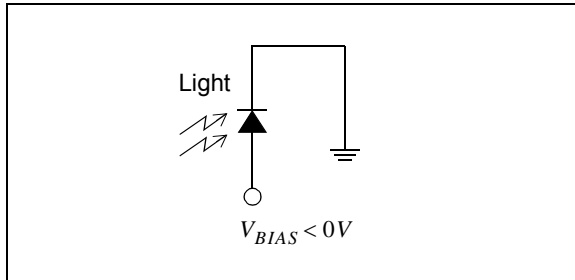


FIGURE 3: Photoconductive Mode.

Photodiode Current-to-Voltage Converter

This circuit is used to convert the photodiode's small output current to a measurable voltage. Typically, there are two types of circuit implementations, which are passive and active versions.

PASSIVE PHOTODIODE CURRENT-TO-VOLTAGE CONVERTER

The Passive Photodiode Current-to-Voltage Converter is implemented by only passive components, as shown in Figure 4. Its output resistance is roughly equal to the value of large resistor (R_F) and the output voltage is equal to $I \cdot R_F$.

The large R_F can cause loading effects for subsequent load resistance and capacitance, such as an inaccurate V_{OUT} and a relatively long response time.

Moreover, the variation of photocurrent can cause the photodiode's biasing voltage to be unstable, which will change the junction capacitance (C_j) and affect the frequency response of photodiode.

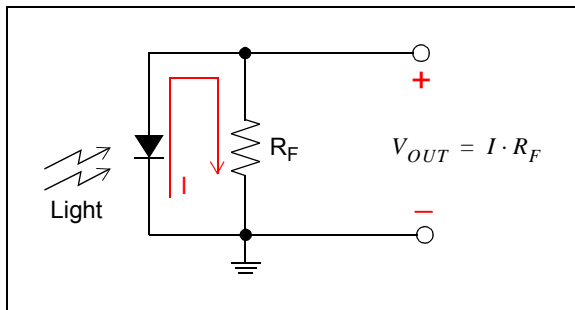


FIGURE 4: Passive Photodiode Current-to-Voltage Converter.

ACTIVE PHOTODIODE CURRENT-TO-VOLTAGE CONVERTER

The active photodiode current-to-voltage converter is also called a photodiode amplifier. Based on the photodiode operating modes, two circuit implementations of photodiode amplifiers are shown in Figure 5 and Figure 6. For the strengths and drawbacks of each implementation, please refer to the section "Operation Modes".

Both implementations have a large resistor (R_F) in the feedback loop. The output resistance of the photodiode amplifier is roughly equal to R_F/A_{OL} , where A_{OL} is the open loop gain of the op amp. Therefore, the output resistance becomes very small and the loading effects can be ignored.

For the photoconductive mode amplifier, the biasing voltage is equal to V_{BIAS} . For the photovoltaic mode amplifier, the biasing voltage is just zero. Both biasing voltages do not change when the photocurrent varies, so the photodiode's frequency response will not be affected.

These strengths of the photodiode amplifier make it widely used in photodetection applications.

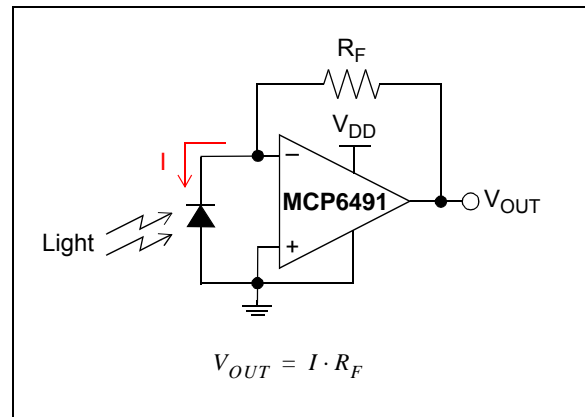


FIGURE 5: "Photovoltaic Mode" Photodiode Amplifier.

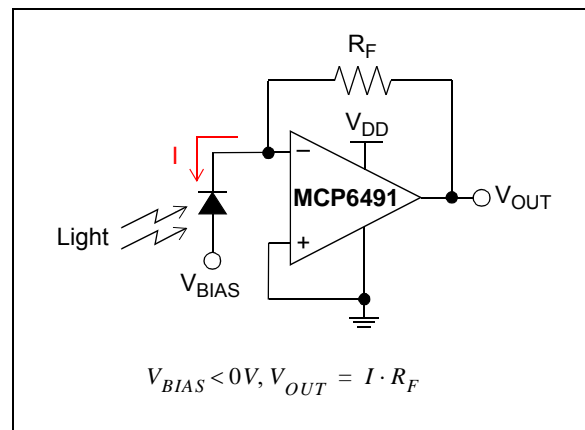


FIGURE 6: "Photoconductive Mode" Photodiode Amplifier.

Photodiode Amplifier Key Design Points

Several key design points for the photodiode amplifier will be analyzed next, in order to improve the circuit's performance.

OP AMP SELECTION

Selecting a suitable op amp for the photodiode amplifier is critical. There are many DC and AC specs in an op amp data sheet, and the key op amp specs for the photodiode amplifier are shown and discussed below.

Low Input Bias Current (I_B)

The DC output voltage error due to I_B is equal to $I_B \cdot R_F$. I_B increases with temperature rise, so the error will be larger at higher temperature. Usually, the voltage error can be reduced to $I_{OS} \cdot R_F$ by adding a compensation resistor R_C with a value of $R_F \parallel R_J$ in series with the op amp non-inverting input.

However, at high temperatures, the value of R_C is difficult to determine because the value of R_J significantly drops with temperature rise. In this condition, the value of R_J could be less than the value of R_F .

Moreover, R_C will develop a noise voltage as the op amp input noise current flows through it. The R_C also generates a thermal noise voltage. Both noise voltages will be amplified by the circuit's noise gain. Thus, the output noise level will increase.

I_B also generates a voltage across R_C at the op amp's non-inverting input. This causes the same voltage at the inverting input. Now, the biasing voltage is no longer stable, which causes the photodiode's response to become nonlinear.

Therefore, adding the compensation resistor R_C to reduce the voltage error $I_B \cdot R_F$ is not an effective method in general. The op amp should have I_B low enough to keep the voltage error within an acceptable range of target applications.

Low Input Offset Voltage (V_{OS})

The DC output voltage error due to V_{OS} is equal to $V_{OS} \cdot (1 + R_F/R_J)$ at room temperature (25°C), which is about V_{OS} because R_F is much less than R_J and the gain is approximately 1 V/V. At high temperatures, the error could be much larger because the value of R_J significantly decreases and the gain can be higher than 1 V/V. Moreover, the V_{OS} drift could make the error even worse. Therefore, low V_{OS} and low V_{OS} drift will be very helpful to reduce the output error at high temperatures.

Common Mode Input Voltage Range

The common mode input voltage range needs to at least include ground because the non-inverting input of the op amp is grounded.

Rail-to-Rail Output

The rail-to-rail output is helpful to maximize the dynamic output voltage range and improve the signal-to-noise ratio (SNR).

Wide Gain Bandwidth Product (GBWP) and High Slew Rate (SR)

The GBWP and SR should be large enough to meet the requirement of output step response time, which will be discussed in more detail later.

Low Input Noise Current Density and Low Input Noise Voltage Density

When noise current flows through the photodiode amplifier, resistor noise voltages will result. The op amp input current noise density ($\sqrt{2qI}$, where q is electron charge, I is current) is determined by I_B , so that lower I_B gives lower op amp input noise current density. The low input noise voltage density also plays a very important role for the output noise of the photodiode amplifier. It will be amplified by the noise gain so that the output noise level will be significantly affected. This will be explained later in this section.

In conclusion, the Microchip's MCP6491 op amp's key features include low I_B , low V_{OS} , low V_{OS} drift with temperature, rail-to-rail input/output, wide GBWP, high SR, low input noise current density and low input noise voltage density, etc. These features make it well suited for the photodiode amplifier.

FEEDBACK RESISTOR

The value of the feedback resistor (R_F) should be set as large as possible to give a high transimpedance gain to the photocurrent. Usually, this gain should be high enough to use most of the op amp's output voltage swing when the photocurrent is at its maximum value. For precision applications, a large resistor with tight tolerance and a low temperature coefficient should be selected.

It is possible to add more gain with subsequent stages, however, the noise performance will not be as good as using a large R_F in one stage, which can easily improve the SNR.

For a given bandwidth Δf , the thermal noise voltage of R_F is given by $\sqrt{4kTR_F\Delta f}$, where k is Boltzmann's constant (1.38×10^{-13} J/K), T is absolute temperature (K), R_F is feedback resistance (Ω).

The output signal is given by $V_{SIGNAL} = I \cdot R_F$ and the $SNR = 20 \cdot \log(V_{SIGNAL}/V_{NOISE})$. When R_F is doubled, the resistor thermal noise voltage is increased by $\sqrt{2}$ and the output signal voltage is increased by 2. Thus, the SNR is increased by 3 dB.

FEEDBACK CAPACITOR

The photodiode amplifier does not always behave as desired. The gain peaking and step output ringing are typical phenomena, which could happen in frequency and time domains (refer to Figure 7 and Figure 8).

Moreover, the noise gain peaking results in very high output noise levels (Figure 9), which may severely degrade the integrity of the output signal.

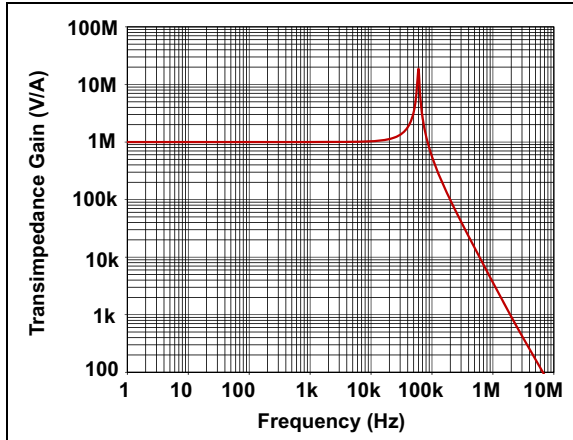


FIGURE 7: Signal Gain (i.e. Transimpedance Gain) Peaking.

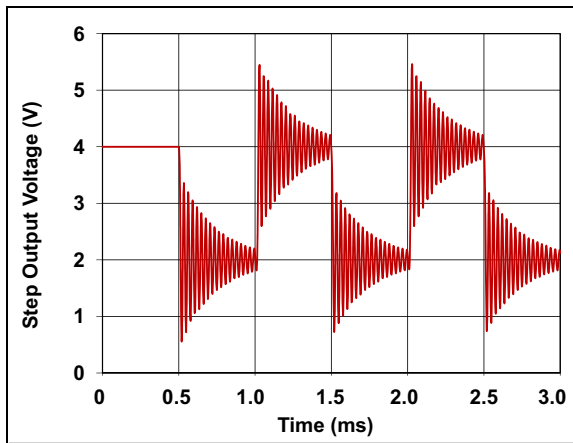


FIGURE 8: Output Ringing.

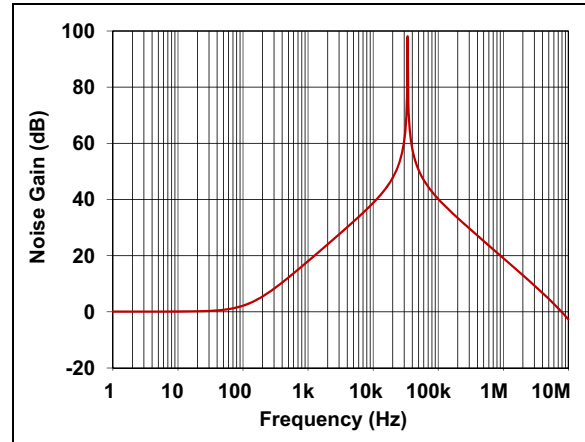


FIGURE 9: Noise Gain Peaking.

These phenomena make the photodiode amplifier unstable. A small capacitor (C_F) can be added in the feedback loop to eliminate the gain peaking, step output ringing and noise gain peaking issues (refer to Figure 10).

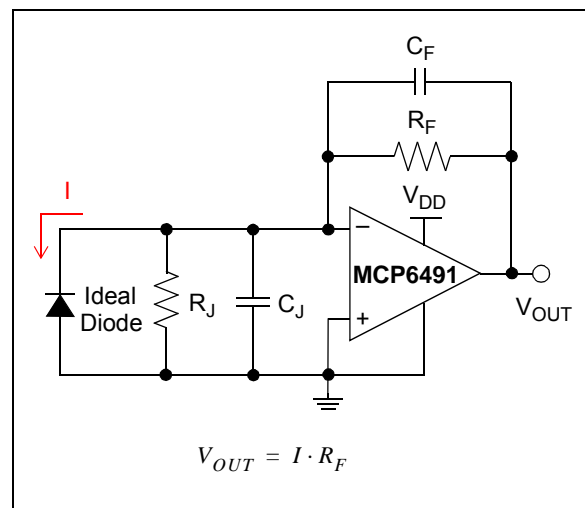


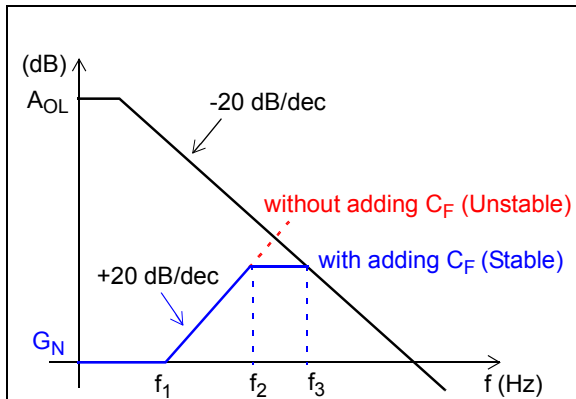
FIGURE 10: Photodiode Amplifier Using Feedback Capacitor.

In the next section, we will discuss the stability of the photodiode amplifier, explain why the amplifier will be stable after adding a feedback capacitor, and learn how to determine the value of the feedback capacitor to get the optimum output response.

AMPLIFIER STABILITY ANALYSIS

Figure 11 shows the noise gain bode plot of the photodiode amplifier in log-log scale. It is important to clarify the difference between the noise gain and the signal gain because the system stability is dependent on the characteristics of noise gain, not signal gain.

The noise gain is the gain seen by a testing voltage source in series with the op amp non-inverting input, which is equal to the signal gain when the signal is applied to the op amp non-inverting input.



$$f_1 = \frac{1}{2\pi \cdot (R_J \parallel R_F) \cdot (C_J + C_{OP} + C_F)}$$

$$f_2 = \frac{1}{2\pi \cdot R_F \cdot C_F}$$

$$f_3 = \frac{GBWP}{G_N} = \frac{GBWP}{1 + \frac{C_J + C_{OP}}{C_F}}$$

Where

R_J = junction shunt resistance

R_F = resistance of feedback resistor

C_J = junction capacitance

C_F = feedback capacitance

C_{OP} = op amp input capacitance

= $C_{CM} + C_{DM}$

C_{CM} = op amp common mode input capacitance

C_{DM} = op amp differential mode input capacitance

GBWP = op amp gain bandwidth product

G_N = noise gain

A_{OL} = op amp open loop gain

f_1 = the location of G_N 's first zero

f_2 = signal gain bandwidth
(i.e. transimpedance gain bandwidth)

f_3 = noise gain bandwidth

The stability of the system is determined by the net slope between the noise gain (G_N) and the open loop gain (A_{OL}) at the frequency where they cross over.

- For an unstable photodiode amplifier, the net slope between G_N and A_{OL} is equal to +40 dB/decade as shown in Figure 11, where the dotted line of G_N intercepts the curve of A_{OL} . The dashed line shows the extended G_N curve without adding C_F .
- For a stable photodiode amplifier, the net slope between G_N and A_{OL} is equal to +20 dB/decade as shown in Figure 11, where the solid line of G_N intercepts the curve of A_{OL} . The solid line shows the G_N curve with adding C_F .

The explanation on the noise gain Bode plot is shown below:

- When f is less than f_1 :
 - G_N is equal to $1 + R_F/R_J$, which is roughly equal to 1 V/V or 0 dB when $R_F \ll R_J$.
 - The zero of G_N is located in f_1 .
- When f is between f_1 and f_2 :
 - G_N increases by +20 dB/dec.
 - The pole of G_N is located in f_2 , which is equal to $1/(2\pi \cdot R_F \cdot C_F)$. This is also the signal gain bandwidth.
- When f is between f_2 and f_3 :
 - G_N is equal to $1 + (C_J + C_{OP})/C_F$.
 - The crossover frequency of A_{OL} and G_N is located in f_3 , which is equal to $GBWP/G_N$.
- When f is larger than f_3 :
 - G_N is determined and limited by A_{OL} , which decreases by -20 dB/dec.

The value of C_F affects the location of f_2 , which determines the signal gain bandwidth and the phase margin of the photodiode amplifier.

When C_F becomes larger, the phase margin will be increased, which makes the system more stable with less gain peaking, step overshoot and noise gain peaking. However, this also will result in smaller signal gain bandwidth and longer output response time.

Table 1 below shows the percent overshoot as a result of different phase margins.

TABLE 1:

Phase Margin (°)	Overshoot (%)
45	25
55	13.3
65	4.7
75	0.008

FIGURE 11: Noise Gain Bode Plot.

For most photodetection applications, the optimum value of C_F is typically considered when the phase margin is 65° , which gives a negligible gain peaking and 4.7% overshoot at output, while keeping reasonable signal gain bandwidth and response time.

The value of C_F at 65° phase margin is approximately shown in Equation 1 where $R_F \ll R_J$ is assumed.

EQUATION 1:

$$C_F \approx 2 \cdot \sqrt{\frac{C_J + C_{OP}}{2\pi \cdot R_F \cdot GBWP}}$$

In Figure 11, the maximum signal gain bandwidth is achieved at 45° phase margin when f_2 is equal to f_3 , and the corresponding value of C_F will be half of the one shown in Equation 1.

If we consider the effect of R_F 's parasitic capacitance, C_F will be the value of the one shown in Equation 1 minus R_F 's parasitic capacitance.

Normally, the parasitic capacitance is less than 0.1 pF for a surface mount resistor due to its small size. Thus, the effect of the parasitic capacitance can be ignored.

APPLICATION EXAMPLE

Here we provide an example to illustrate the circuit's performance improvement in frequency and time domains after the feedback capacitor is added.

In Figure 12, the photodiode's $R_J = 2000 \text{ M}\Omega$ at 25°C , $C_J = 100 \text{ pF}$, MCP6491 op amp's $V_{DD} = 5.5\text{V}$, $R_F = 10 \text{ M}\Omega$, and assume V_{OUT} switches between 2V and 4V for the two alternating illumination levels.

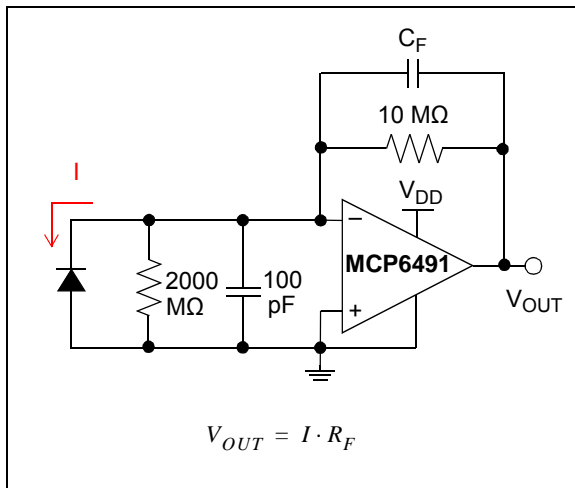


FIGURE 12: Photodiode Amplifier Circuit Example.

MCP6491 op amp's typical GBWP is 7.5 MHz and its input capacitance is $C_{OP} = C_{CM} + C_{DM} = 12 \text{ pF}$.

To make the photodiode amplifier stable, a feedback capacitor C_F is needed. Based on Equation 1, the value of C_F is 1 pF when the amplifier's phase margin is 65° .

At room temperature (25°C), the DC voltage error at output due to I_B and V_{OS} of MCP6491 is given by $I_B \cdot R_F + V_{OS} = 1 \text{ pA} \cdot 10 \text{ M}\Omega + 1.5 \text{ mV} = 1.51 \text{ mV}$.

The graphs in Figure 13 — Figure 17 show the related output response plots with and without adding C_F .

Note: These plots are PSpice simulation results by using MCP6491 op amp Spice macro model, which is free on the Microchip web site at www.microchip.com. The model is intended to be an initial design tool. Bench testing is a very important part of any design and cannot be replaced with simulations.

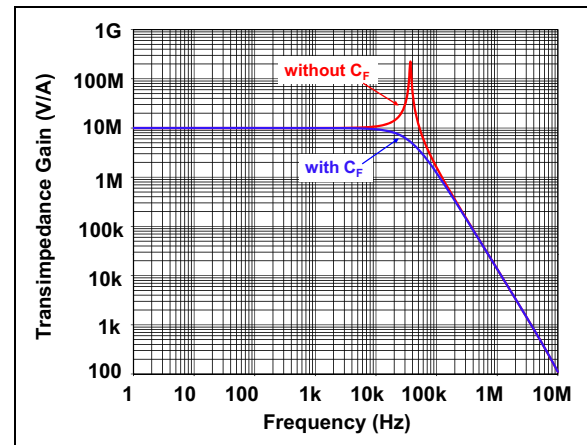


FIGURE 13: Signal Gain vs. Frequency.

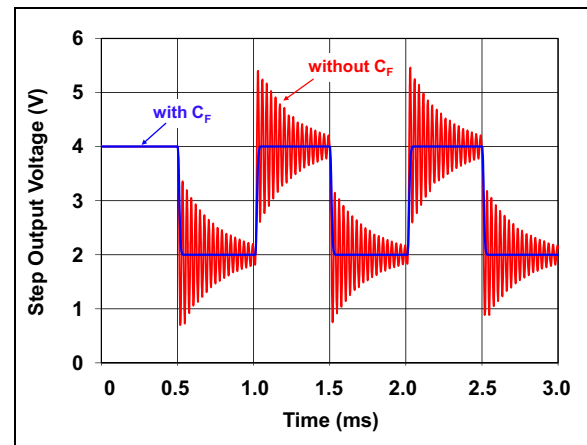


FIGURE 14: Step Output Response.

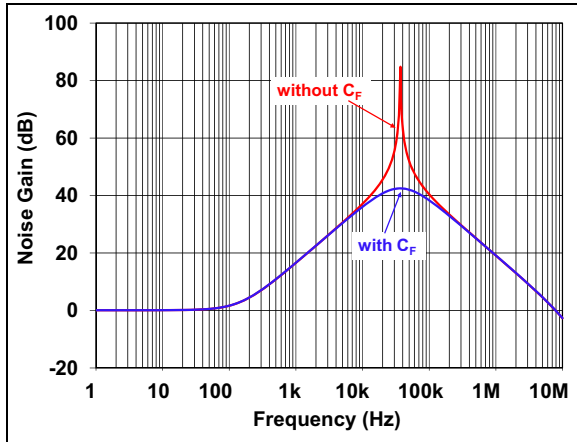


FIGURE 15: Noise Gain vs. Frequency.

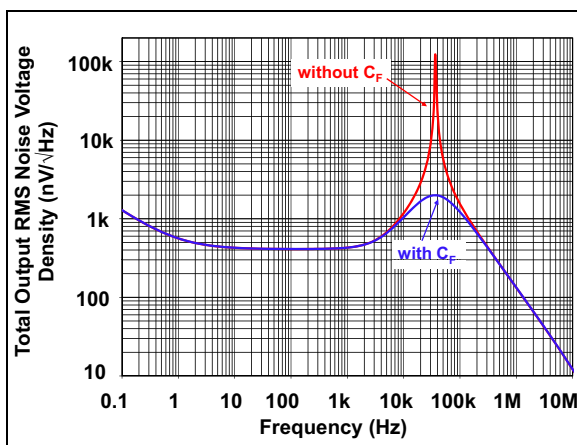


FIGURE 16: Total Output RMS Noise Voltage Density vs. Frequency.

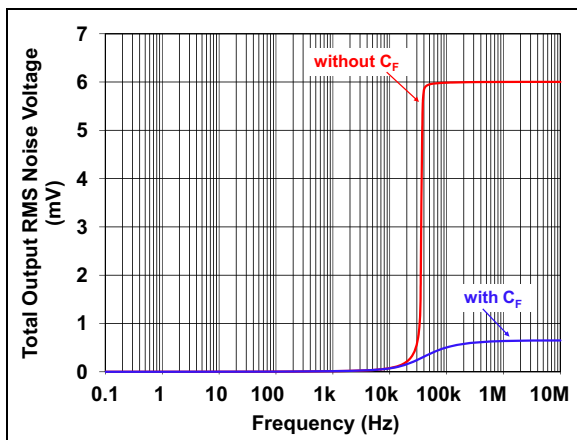


FIGURE 17: Total Output RMS Noise Voltage vs. Frequency.

Although the added C_F eliminates a lot of output noise, we still need to further reduce the noise in order to improve the SNR and achieve better signal integrity. Now we will focus on the noise analysis of the photodiode amplifier.

Photodiode Amplifier Noise Analysis

Figure 18 shows the noise model of the photodiode amplifier.

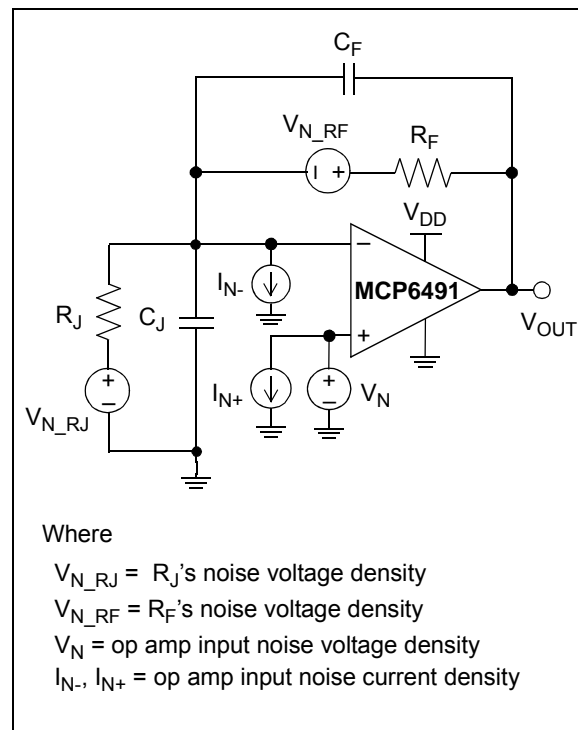


FIGURE 18: Noise Model.

Two ways to quickly estimate total output root-mean-square (RMS) noise are provided:

- Hand Calculation
- PSpice Simulation

NOISE ESTIMATED BY HAND CALCULATION

The resistor voltage noise density is given by $V_N = \sqrt{4kTR}$ and is spectrally flat. For a 1 k Ω resistor, the V_N is 4 nV/ $\sqrt{\text{Hz}}$.

The typical input noise voltage density and input noise current density of MCP6491 are 19 nV/ $\sqrt{\text{Hz}}$ and 0.6 fA/ $\sqrt{\text{Hz}}$, respectively. The input noise voltage density vs. frequency plot can be found in the MCP6491 data sheet. The 1/f noise is dominant in the lower frequencies while the thermal noise is dominant in the higher frequencies.

The total output RMS noise is calculated by the square root of the sum of the squared values of the individual output noise contributors. Each output noise contributor is calculated by integrating its squared output noise density over the equivalent noise bandwidth in a square root. The output noise density is calculated by multiplying its input noise density by an appropriate gain. Note that the worst output noise contributor will dominate the total output RMS noise.

Table 2 shows the input noise density of each noise source, the corresponding output noise density and the equivalent noise bandwidth.

For a single pole system, the equivalent noise bandwidth is equal to the -3 dB bandwidth multiplied by 1.57. Because there is no resistor in series with the op amp's non-inverting input, I_{N+} does not contribute to output noise.

TABLE 2:

Input Noise Density	Output Noise Density	Equivalent Noise Bandwidth
V_N	$V_N * G_N$	1.57*Noise Gain Bandwidth
I_{N-}	$I_{N-} * R_F$	1.57*Signal Gain Bandwidth
$V_{N_{RJ}}$	$V_{N_{RJ}} * (R_F/R_J)$	1.57*Signal Gain Bandwidth
$V_{N_{RF}}$	$V_{N_{RF}}$	1.57*Signal Gain Bandwidth

Note 1: The noise gain bandwidth is given by $GBWP/G_N$.

2: The signal gain bandwidth is given by $1/(2\pi * R_F * C_F)$.

For the circuit shown in Figure 12, the noise gain bandwidth is $(7.5 \text{ MHz})/(113 \text{ V/V}) = 66 \text{ kHz}$ and its equivalent noise bandwidth is $66 \text{ kHz} * 1.57 = 104 \text{ kHz}$. The signal gain bandwidth is 16 kHz and its equivalent noise bandwidth is $16 \text{ kHz} * 1.57 = 25 \text{ kHz}$.

The G_N is dependent on frequency; it is 1 V/V at lower frequencies and gradually becomes higher with a maximum of 113 V/V at higher frequencies. Instead of integrating G_N over frequency, we simply use 113 V/V as the noise gain over the equivalent noise bandwidth for quick noise estimation.

Thus, the output noise from each contributor can be estimated, according to Table 2, and the results are shown in Table 3.

TABLE 3:

Input Noise Density	Output Noise Voltage Density (nV/ $\sqrt{\text{Hz}}$)	Individual Output Noise Voltage (RMS in μV)
V_N	$V_N * G_N = 19 * 113$	692
I_{N-}	$I_{N-} * R_F = 6$	1
$V_{N_{RJ}}$	$V_{N_{RJ}} * (R_F/R_J) = 28$	4.4
$V_{N_{RF}}$	$V_{N_{RF}} = 400$	63

The total output RMS noise is equal to $695 \mu\text{V}$, which is the square root of the sum of the individual squared output noise values.

Notice that the op amp's input noise voltage density (V_N) needs to be multiplied by noise gain G_N to get the corresponding output noise density, and the noise gain bandwidth is much larger than the signal gain bandwidth. This makes V_N dominate the total output RMS noise voltage.

NOISE ESTIMATED BY PSpICE SIMULATION

Figure 19 shows the MCP6491 op amp input noise voltage density spectrum simulation plot by using the MCP6491 op amp Spice macro model in PSpice, which matches the noise density spectrum plot of MCP6491 data sheet well.

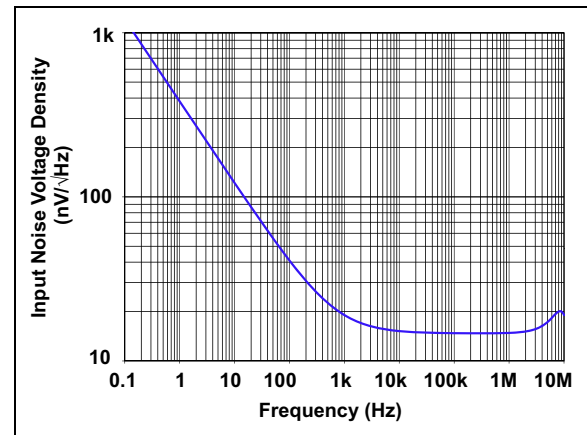


FIGURE 19: MCP6491 Op Amp Input Noise Voltage Density vs. Frequency.

Figure 20 shows the total output RMS noise voltage density spectrum.

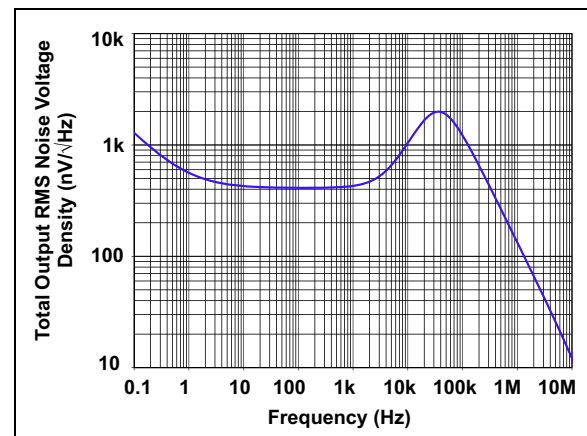


FIGURE 20: Total Output RMS Noise Voltage Density vs. Frequency.

Figure 21 shows the total output RMS noise voltage spectrum. Within 10 MHz, the total output RMS noise voltage is 650 μV .

The noise estimated by hand calculation (695 μV) is similar to the one simulated by PSpice.

For a 4V output voltage signal, the SNR is equal to $20 \cdot \log(V_{\text{SIGNAL}}/V_{\text{NOISE}}) = 20 \cdot \log(4\text{V}/650\mu\text{V}) = 76 \text{ dB}$.

Note: In PSpice probe, the trace expression "SQRT(S(V(ONoise)*V(ONoise)))" can be used to integrate output noise voltage density over bandwidth.

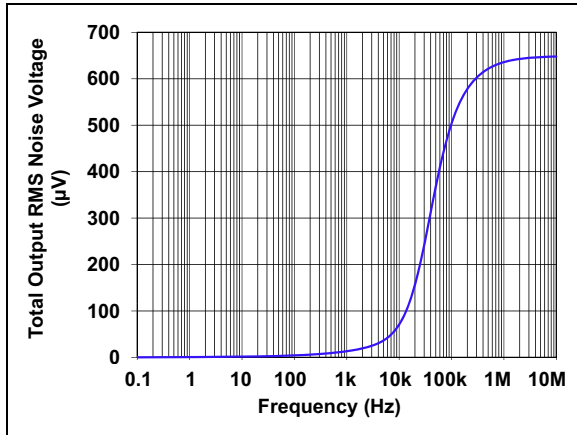


FIGURE 21: Total Output RMS Noise Voltage vs. Frequency.

NOISE FILTERING

In Figure 22, a single pole RC low pass filter can follow the photodiode amplifier to eliminate the noise beyond the signal gain bandwidth.

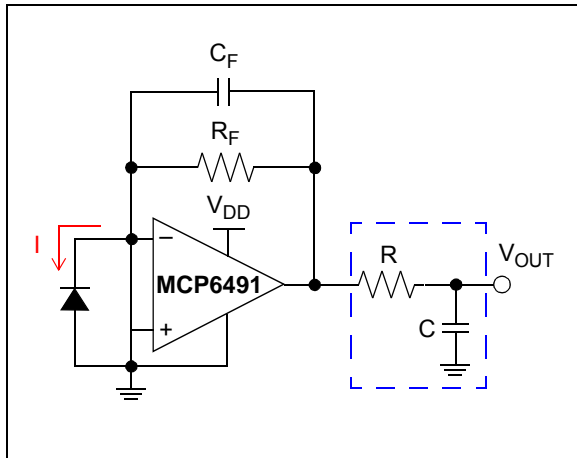


FIGURE 22: Noise Filtering.

In Equation 2, the low pass filter's cut-off frequency (f_c) is set to be equal to the maximum allowed signal gain, which gives the minimum rising time (t_R) of the output step.

For a fixed R_F , t_R can be further reduced by choosing an op amp with higher GBWP. The higher GBWP makes the value of C_F smaller based on Equation 1, and thus makes f_c larger.

EQUATION 2:

$$f_c = \frac{1}{2\pi \cdot R_F \cdot C_F}$$

$$t_R \approx \frac{0.35}{f_c}$$

Where

f_c = cut-off frequency of low pass filter

t_R = 10% to 90% rising time (s)

As shown in Figure 12, $R_F = 10 \text{ M}\Omega$, $C_F = 1 \text{ pF}$, thus f_c is 16 kHz and t_R is 22 μs based on Equation 2.

In Figure 23, the step output responses are shown for the low pass filters with different f_c . Notice that the filter with lower f_c yields longer t_R .

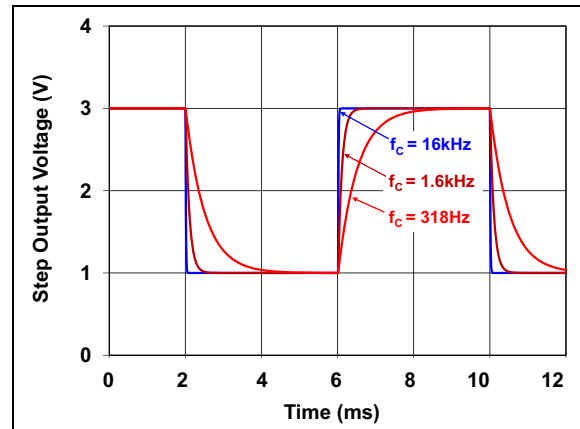


FIGURE 23: Step Output Response vs. Low Pass Filter's f_c .

The low pass filter also serves as an anti-aliasing filter for the subsequent analog-to-digital converter (ADC). The ADC's sampling rate should be at least two times of the low pass filter's f_c .

We chose $R = 100\text{ k}\Omega$ and $C = 0.1\text{ nF}$ to make the low pass filter with $f_c = 16\text{ kHz}$. The noise generated by the filter itself is negligible.

In [Figure 24](#) and [Figure 25](#), the related output RMS noise spectrum plots with and without filtering are shown, which are PSpice simulation results.

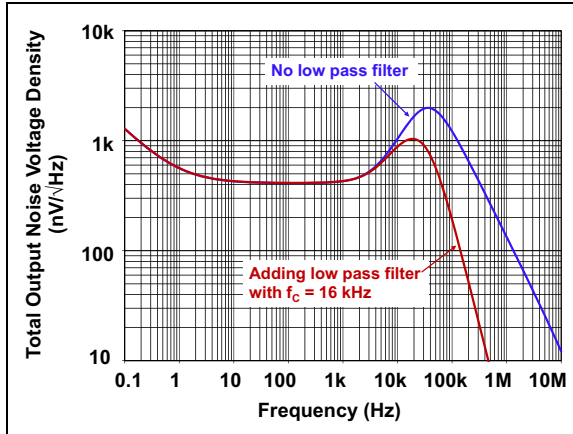


FIGURE 24: Total Output RMS Noise Voltage Density vs. Frequency.

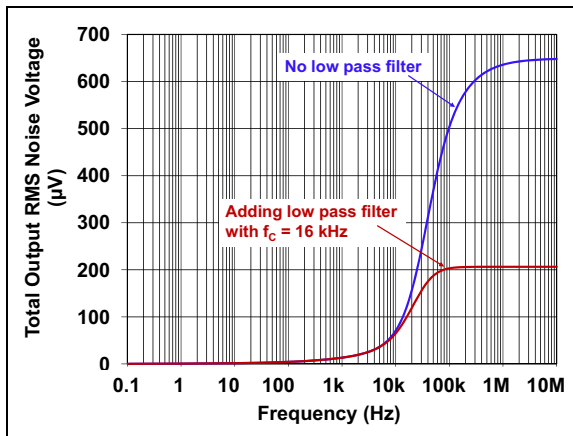


FIGURE 25: Total Output RMS Noise Voltage vs. Frequency.

In [Figure 25](#), the total output RMS noise voltage is $205\text{ }\mu\text{V}$ within 10 MHz .

For a 4 V output voltage signal, the SNR is equal to $20 \cdot \log(V_{\text{SIGNAL}}/V_{\text{NOISE}}) = 20 \cdot \log(4\text{ V}/205\text{ }\mu\text{V}) = 86\text{ dB}$, which is 10 dB higher than the SNR without filtering.

PCB Surface Leakage

In photodetection applications, PCB surface leakage effects need to be considered. Surface leakage is caused by humidity, dust or other contamination on the board. Under low-humidity conditions, a typical resistance between nearby traces is $10^{12}\text{ }\Omega$. A 5 V difference would cause 5 pA of current to flow, which is greater than the MCP6491 family's bias current at $+25^\circ\text{C}$ (1 pA , typical).

There are several ways to reduce surface leakage such as cleaning, coating and guard rings.

Cleaning with isopropyl alcohol helps remove residues, and coating isolates the surface from moisture, dust, etc.

The more reliable and permanent solution to reduce surface leakage is using guard rings. As shown in [Figure 26](#), the guard ring drawn in the dotted line is a low impedance conductive trace and it surrounds the sensitive inverting input pin area. The guard ring is biased at the same voltage as the sensitive inverting input pin so that there is no leakage current between itself and the guarded sensitive pin. In a photodiode amplifier circuit, the guard ring is directly connected to the op amp's grounded non-inverting input pin. Thus, the guard ring blocks the leakage current which would flow into the sensitive pin, and sinks it to ground. Moreover, to minimize coupling effects, the circuit connections within the guard ring should be kept as short as possible.

For more information on PCB layout techniques, please refer to Microchip's AN1258 ("Op Amp Precision Design: PCB Layout Techniques").

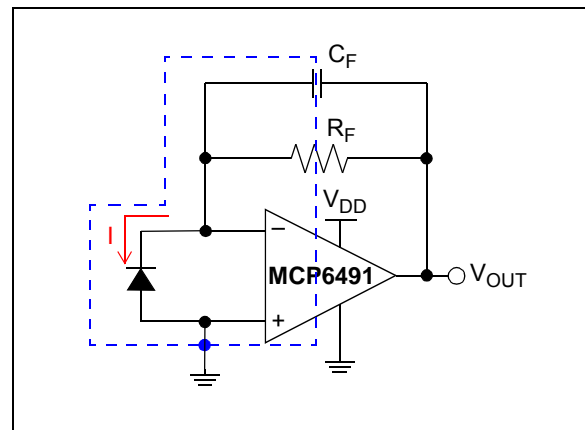


FIGURE 26: Guard Ring Technique.

SUMMARY

This application note reviews the features of Microchip's MCP6491 low input bias current op amps [1], the characteristics and operation modes of photodiodes, then it focuses on designing photodiode amplifier circuitry, and several key design points are discussed in order to improve the circuit's performance. The noise analysis of a photodiode amplifier and the design technique of a low pass filter are also discussed. Finally, the PCB techniques that help reduce the current leakage are briefly introduced as well.

REFERENCES

- [1] MCP6491 Data Sheet, "7.5 MHz Low Input Bias Current Op Amps", Microchip Technology Inc., DS22321, 2012
- [2] MCP6481 Data Sheet, "4 MHz Low Input Bias Current Op Amps", Microchip Technology Inc., DS22322, 2012
- [3] MCP6471 Data Sheet, "2 MHz Low Input Bias Current Op Amps", Microchip Technology Inc., DS22324, 2012

Note the following details of the code protection feature on Microchip devices:

- Microchip products meet the specification contained in their particular Microchip Data Sheet.
- Microchip believes that its family of products is one of the most secure families of its kind on the market today, when used in the intended manner and under normal conditions.
- There are dishonest and possibly illegal methods used to breach the code protection feature. All of these methods, to our knowledge, require using the Microchip products in a manner outside the operating specifications contained in Microchip's Data Sheets. Most likely, the person doing so is engaged in theft of intellectual property.
- Microchip is willing to work with the customer who is concerned about the integrity of their code.
- Neither Microchip nor any other semiconductor manufacturer can guarantee the security of their code. Code protection does not mean that we are guaranteeing the product as “unbreakable.”

Code protection is constantly evolving. We at Microchip are committed to continuously improving the code protection features of our products. Attempts to break Microchip's code protection feature may be a violation of the Digital Millennium Copyright Act. If such acts allow unauthorized access to your software or other copyrighted work, you may have a right to sue for relief under that Act.

Information contained in this publication regarding device applications and the like is provided only for your convenience and may be superseded by updates. It is your responsibility to ensure that your application meets with your specifications. MICROCHIP MAKES NO REPRESENTATIONS OR WARRANTIES OF ANY KIND WHETHER EXPRESS OR IMPLIED, WRITTEN OR ORAL, STATUTORY OR OTHERWISE, RELATED TO THE INFORMATION, INCLUDING BUT NOT LIMITED TO ITS CONDITION, QUALITY, PERFORMANCE, MERCHANTABILITY OR FITNESS FOR PURPOSE. Microchip disclaims all liability arising from this information and its use. Use of Microchip devices in life support and/or safety applications is entirely at the buyer's risk, and the buyer agrees to defend, indemnify and hold harmless Microchip from any and all damages, claims, suits, or expenses resulting from such use. No licenses are conveyed, implicitly or otherwise, under any Microchip intellectual property rights.

Trademarks

The Microchip name and logo, the Microchip logo, dsPIC, FlashFlex, KEELOQ, KEELOQ logo, MPLAB, PIC, PICmicro, PICSTART, PIC³² logo, rPIC, SST, SST Logo, SuperFlash and UNI/O are registered trademarks of Microchip Technology Incorporated in the U.S.A. and other countries.

FilterLab, Hampshire, HI-TECH C, Linear Active Thermistor, MTP, SEEVAL and The Embedded Control Solutions Company are registered trademarks of Microchip Technology Incorporated in the U.S.A.

Silicon Storage Technology is a registered trademark of Microchip Technology Inc. in other countries.

Analog-for-the-Digital Age, Application Maestro, BodyCom, chipKIT, chipKIT logo, CodeGuard, dsPICDEM, dsPICDEM.net, dsPICworks, dsSPEAK, ECAN, ECONOMONITOR, FanSense, HI-TIDE, In-Circuit Serial Programming, ICSP, Mindi, MiWi, MPASM, MPF, MPLAB Certified logo, MPLIB, MPLINK, mTouch, Omniclient Code Generation, PICC, PICC-18, PICDEM, PICDEM.net, PICkit, PICtail, REAL ICE, rLAB, Select Mode, SQI, Serial Quad I/O, Total Endurance, TSHARC, UniWinDriver, WiperLock, ZENA and Z-Scale are trademarks of Microchip Technology Incorporated in the U.S.A. and other countries.

SQTP is a service mark of Microchip Technology Incorporated in the U.S.A.

GestIC and ULPP are registered trademarks of Microchip Technology Germany II GmbH & Co. & KG, a subsidiary of Microchip Technology Inc., in other countries.

All other trademarks mentioned herein are property of their respective companies.

© 2013, Microchip Technology Incorporated, Printed in the U.S.A., All Rights Reserved.

 Printed on recycled paper.

ISBN: 978-1-62076-987-4

QUALITY MANAGEMENT SYSTEM
CERTIFIED BY DNV
== ISO/TS 16949 ==

Microchip received ISO/TS-16949:2009 certification for its worldwide headquarters, design and wafer fabrication facilities in Chandler and Tempe, Arizona; Gresham, Oregon and design centers in California and India. The Company's quality system processes and procedures are for its PIC[®] MCUs and dsPIC[®] DSCs, KEELOQ[®] code hopping devices, Serial EEPROMs, microperipherals, nonvolatile memory and analog products. In addition, Microchip's quality system for the design and manufacture of development systems is ISO 9001:2000 certified.



MICROCHIP

Worldwide Sales and Service

AMERICAS

Corporate Office
2355 West Chandler Blvd.
Chandler, AZ 85224-6199
Tel: 480-792-7200
Fax: 480-792-7277
Technical Support:
<http://www.microchip.com/support>
Web Address:
www.microchip.com

Atlanta
Duluth, GA
Tel: 678-957-9614
Fax: 678-957-1455

Boston
Westborough, MA
Tel: 774-760-0087
Fax: 774-760-0088

Chicago
Itasca, IL
Tel: 630-285-0071
Fax: 630-285-0075

Cleveland
Independence, OH
Tel: 216-447-0464
Fax: 216-447-0643

Dallas
Addison, TX
Tel: 972-818-7423
Fax: 972-818-2924

Detroit
Farmington Hills, MI
Tel: 248-538-2250
Fax: 248-538-2260

Indianapolis
Noblesville, IN
Tel: 317-773-8323
Fax: 317-773-5453

Los Angeles
Mission Viejo, CA
Tel: 949-462-9523
Fax: 949-462-9608

Santa Clara
Santa Clara, CA
Tel: 408-961-6444
Fax: 408-961-6445

Toronto
Mississauga, Ontario,
Canada
Tel: 905-673-0699
Fax: 905-673-6509

ASIA/PACIFIC

Asia Pacific Office
Suites 3707-14, 37th Floor
Tower 6, The Gateway
Harbour City, Kowloon
Hong Kong
Tel: 852-2401-1200
Fax: 852-2401-3431

Australia - Sydney
Tel: 61-2-9868-6733
Fax: 61-2-9868-6755

China - Beijing
Tel: 86-10-8569-7000
Fax: 86-10-8528-2104

China - Chengdu
Tel: 86-28-8665-5511
Fax: 86-28-8665-7889

China - Chongqing
Tel: 86-23-8980-9588
Fax: 86-23-8980-9500

China - Hangzhou
Tel: 86-571-2819-3187
Fax: 86-571-2819-3189

China - Hong Kong SAR
Tel: 852-2943-5100
Fax: 852-2401-3431

China - Nanjing
Tel: 86-25-8473-2460
Fax: 86-25-8473-2470

China - Qingdao
Tel: 86-532-8502-7355
Fax: 86-532-8502-7205

China - Shanghai
Tel: 86-21-5407-5533
Fax: 86-21-5407-5066

China - Shenyang
Tel: 86-24-2334-2829
Fax: 86-24-2334-2393

China - Shenzhen
Tel: 86-755-8864-2200
Fax: 86-755-8203-1760

China - Wuhan
Tel: 86-27-5980-5300
Fax: 86-27-5980-5118

China - Xian
Tel: 86-29-8833-7252
Fax: 86-29-8833-7256

China - Xiamen
Tel: 86-592-2388138
Fax: 86-592-2388130

China - Zhuhai
Tel: 86-756-3210040
Fax: 86-756-3210049

ASIA/PACIFIC

India - Bangalore
Tel: 91-80-3090-4444
Fax: 91-80-3090-4123

India - New Delhi
Tel: 91-11-4160-8631
Fax: 91-11-4160-8632

India - Pune
Tel: 91-20-2566-1512
Fax: 91-20-2566-1513

Japan - Osaka
Tel: 81-6-6152-7160
Fax: 81-6-6152-9310

Japan - Tokyo
Tel: 81-3-6880-3770
Fax: 81-3-6880-3771

Korea - Daegu
Tel: 82-53-744-4301
Fax: 82-53-744-4302

Korea - Seoul
Tel: 82-2-554-7200
Fax: 82-2-558-5932 or
82-2-558-5934

Malaysia - Kuala Lumpur
Tel: 60-3-6201-9857
Fax: 60-3-6201-9859

Malaysia - Penang
Tel: 60-4-227-8870
Fax: 60-4-227-4068

Philippines - Manila
Tel: 63-2-634-9065
Fax: 63-2-634-9069

Singapore
Tel: 65-6334-8870
Fax: 65-6334-8850

Taiwan - Hsin Chu
Tel: 886-3-5778-366
Fax: 886-3-5770-955

Taiwan - Kaohsiung
Tel: 886-7-213-7828
Fax: 886-7-330-9305

Taiwan - Taipei
Tel: 886-2-2508-8600
Fax: 886-2-2508-0102

Thailand - Bangkok
Tel: 66-2-694-1351
Fax: 66-2-694-1350

EUROPE

Austria - Wels
Tel: 43-7242-2244-39
Fax: 43-7242-2244-393

Denmark - Copenhagen
Tel: 45-4450-2828
Fax: 45-4485-2829

France - Paris
Tel: 33-1-69-53-63-20
Fax: 33-1-69-30-90-79

Germany - Munich
Tel: 49-89-627-144-0
Fax: 49-89-627-144-44

Italy - Milan
Tel: 39-0331-742611
Fax: 39-0331-466781

Netherlands - Drunen
Tel: 31-416-690399
Fax: 31-416-690340

Spain - Madrid
Tel: 34-91-708-08-90
Fax: 34-91-708-08-91

UK - Wokingham
Tel: 44-118-921-5869
Fax: 44-118-921-5820

11/29/12